Refined RBF-FD Solution of Linear Elasticity Problem

Jure Slak
"Jožef Stefan" Institute
Parallel and Distributed Systems Laboratory,
Jamova cesta 39, 1000 Ljubljana, Slovenia
Email: jure.slak@ijs.si

Gregor Kosec
"Jožef Stefan" Institute
Parallel and Distributed Systems Laboratory,
Jamova cesta 39, 1000 Ljubljana, Slovenia
Email: gregor.kosec@ijs.si

***Abstract*—Solving PDEs with Radial Basis Functions, especially using local approaches, has become a promising alternative to the Finite Element Method. This paper describes one such approach, a local RBF-FD method, analogous to Finite Difference Method, that can handle irregular geometries, varying discretization densities and is easy to implement. RBF-FD method is analysed by solving basic linear elasticity problems using uniform and refined discretizations. Finally, a linear elasticity problem arising from analysis of fretting fatigue is solved and RBF-FD solution is compared to existing solutions, obtained using commercial software.**

I. Introduction

Radial basis functions (RBFs) arose in scattered data interpolation and surface reconstruction in the 70s [1]. Their wide acceptance followed as a consequence of important non-singularity result by Micchelli [2]. Since then, the theoretical foundations surrounding RBFs have matured and have been summarized in various monographs, eg. by Buhmann [3]. Kansa was the first to suggest in 1990 [4], [5] that RBFs could be used for derivative approximation and for development of numerical methods for solving partial differential equations (PDEs). First, global collocation methods involving RBFs were developed [6], exhibiting good convergence properties. However, since the cost of the global approach scales as $O(N^3)$, where N represents the number of nodes, research focus has shifted towards local approximations. Other local approximations, generalizing Finite Difference (FD) approximations to scattered and irregular node distributions, have been developed in the meantime, most notably Finite Point Method [7] and other Weighted or Moving Least Squares approximations using monomials. Many of these types of approximations however suffer from Mairhuber–Curtis theorem [8], [9], which states that there will inevitably exist infinitely many singular node configurations in two and higher-dimensional domains. This increased the popularity of RBF-based approximations even further, and local schemes generalizing FD approach were developed among others by Tolstykh [10]. Both global and local approaches have since been successfully used for large scale simulations as described by Fornberg and Flyer [11] in their review article. This paper extends the range of examples to linear elasticity problems arising from fretting fatigue, by using RBF-FD method to solve the problem described and solved by Pereira et al. [12]. This paper also extends previous work [13] in this area that dealt with extensively refined discretizations on cases with known closed form solutions to more realistic cases.

The rest of the paper is organized as follows: in section II RBF-FD methodology is explained, in section III the governing equations along with analyses of the standard cantilever beam problem are presented, in section IV the case arising from fretting fatigue is presented and finally, the paper offers some conclusions and directions for future work in the last section.

II. Method description

A. Radial basis functions

Radial basis functions over a set of nodes $X = \{x_1, \dots x_n\}$ generated by a radial function $\phi\colon [0, \infty) \to \mathbb{R}$ are functions

$$\{\phi_i := \phi(\| \cdot - x_i\|), \text{ for } x_i \in X\}. \tag{1}$$

Common radial basis functions include (writing $r = \|x - x_i\|$) Gaussians:

$$\phi_i(x) = \exp(-(\varepsilon r)^2), \tag{2}$$

multiquadrics:

$$\phi_i(x) = \sqrt{1 + (\varepsilon r)^2}, \tag{3}$$

and polyharmonic splines:

$$\phi(r) = r^k, \ k \text{ odd}, \quad \phi(r) = r^k \ln(r), \ k \text{ even}. \tag{4}$$

Many other types are known and used, with different recommendations. The reader is referred to [3] for more information. The parameter ε (where present) is called the shape parameter and characterizes flatness of radial basis functions. In this paper, Gaussian radial basis functions (Fig. 1) will be used.

B. Solution procedure

Consider an elliptic problem with Dirichlet boundary conditions

$$\begin{aligned} \mathcal{L}u &= f \quad \text{on } \Omega \\ u &= u_0 \quad \text{on } \partial\Omega, \end{aligned}$$

where f and u_0 are known functions. The domain Ω is discretized using N nodes, N_i nodes in the interior and N_b nodes on the boundary. Each node x_i is assigned n_i

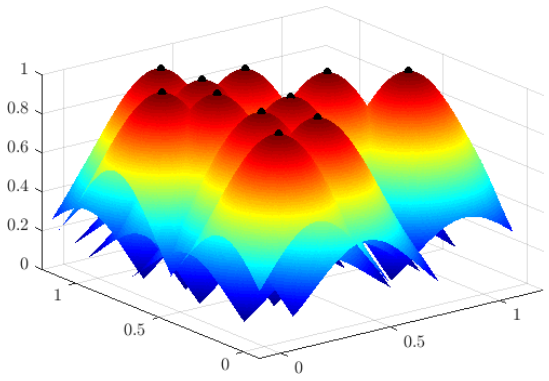

Fig. 1: Gaussian radial basis functions with $\varepsilon = 3$ over a set of randomly generated nodes.

neighbours, denoted $N(x_i)$, that constitute its stencil. The word stencil is used to keep terminology similar to FD method, but *support domain* or *neighborhood* are often used as well, as the neighbours have potentially different arrangements at every node and therefore have little similarities to actual stencils.

In one dimensional FD case, the well known stencil weights for second derivative approximation on equispaced grid with spacing h are $[1/h^2, -2/h^2, 1/h^2]$, giving the approximation

$$u''(x) \approx \frac{1}{h^2}u(x-h) - \frac{2}{h^2}u(x) + \frac{1}{h^2}u(x+h). \tag{5}$$

These weights are known in advance and are assembled in a global sparse system, which is then solved to obtain a numerical approximation for values of u at points x_i. RBF-FD method uses the same technique, except that the stencil weights cannot be known beforehand in general, but rather need to be computed as part of the solution procedure. Similarly to FD method, the operator $\mathcal{L}$ is approximated as a weighted linear combination of function values at stencil points

$$(\mathcal{L}u)(x_i) \approx \sum_{x_j \in N(x_i)} w_j^i u(x_j). \tag{6}$$

To determine the weights w_j^i, exactness of (6) is imposed for a certain set of functions. In FD method, exactness is required for monomials, in RBF-FD method, exactness for radial basis functions is required, yielding equations

$$(\mathcal{L}\phi_k)(x_i) = \sum_{x_j \in N(x_i)} w_j^i \phi_k(x_j), \tag{7}$$

for all $x_k \in N(x_i)$. Rewriting (7) in matrix form, one obtains

$$\begin{bmatrix} \phi(\|x_{j_1} - x_{j_1}\|) & \cdots & \phi(\|x_{j_{n_i}} - x_{j_1}\|) \\ \vdots & \ddots & \vdots \\ \phi(\|x_{j_1} - x_{j_{n_i}}\|) & \cdots & \phi(\|x_{j_{n_i}} - x_{j_{n_i}}\|) \end{bmatrix} \begin{bmatrix} w_{j_1}^i \\ \vdots \\ w_{j_{n_i}}^i \end{bmatrix} = \begin{bmatrix} (\mathcal{L}\phi_{j_1})(x_i) \\ \vdots \\ (\mathcal{L}\phi_{j_{n_i}})(x_i) \end{bmatrix}, \tag{8}$$

where j_k are indices of nodes in $N(x_i)$. This is a system of n_i linear equations, compactly written as $A_i w_i = b_i$, where matrix A_i is symmetric. Furthermore, when using Gaussian basis functions, it can be proven [11] that A_i is positive definite (and therefore nonsingular) as soon as all stencil nodes are distinct.

After computing the weight vectors w_i for all nodes, the weights are assembled in a sparse matrix, right hand side is computed from given f and u_0 and the sparse system is solved to obtain an approximation for u. Vector equations are treated similarly, except that the final system is proportionally larger, since a vector PDE is treated as a coupled system of scalar PDEs. Boundary conditions that involve differential operators, such as Neumann or traction boundary conditions, are also discretized using RBF-FD procedure, analogously to operator $\mathcal{L}$ above.

C. Remarks on weight computation

Often, the RBF-FD approximation is augmented with monomials, to ensure consistency up to a certain order. These consistency constraints are usually enforced using Lagrangian multipliers. The effects of adding polynomial constraints to RBF-FD approximations have been studied recently by Bayona et al. [14]. In the cases discussed in this paper, additional consistency constraints were not needed to obtain satisfying results.

Another possible modification is to include more stencil points then basis functions, putting basis functions only on the closest m_i nodes. This turns (8) into an underdetermined system, however, it can be solved uniquely by imposing additional condition of minimizing the norm $\|w_i\|$ of the weights. This approach was tried by the authors, and the results were very similar, to the ones presented later, so they are not included.

As the shape parameter ε tends towards 0, the matrices A_i become more and more ill conditioned. One solution is to scale the shape parameter ε inversely proportionally to the internodal distance. This however may cause stagnation errors and failure of convergence [15]. Stable algorithms for computation of stencil weights w_i without scaling the shape parameter, such as RBF-QR [16] have been developed to mitigate this issue, however it turned out to not be necessary in this case, as shape scaling performed well enough.

III. Cauchy-Navier equation and the Cantilever Beam problem

The theory of linear elasticity describes stresses and displacement of elastic materials under appropriate loading conditions. The governing equation for homogeneous isotropic materials, suitable for strong form methods, is the Cauchy-Navier equation

$$(\lambda + \mu)\nabla(\nabla \cdot \vec{u}) + \mu\nabla^2\vec{u} = \vec{f}, \tag{9}$$

where $\vec{u}$ are unknown displacements, $\vec{f}$ is the loading body force, and λ and μ are material constants, called Lamé parameters. They are more often expressed in terms of Young's modulus E and Poisson's ratio ν, and the conversion formulas between these quantities (and many others) are well known

and stated in eg. [17, pp. 215]. Another important quantity of interest is the stress tensor σ,

$$\sigma = \lambda \operatorname{tr}(\varepsilon) I + 2\mu\varepsilon, \quad \varepsilon = \frac{\nabla\vec{u} + (\nabla\vec{u})^{\mathsf{T}}}{2}, \tag{10}$$

where λ and μ are Lamé parameters from above and I is the identity tensor.

Two types of boundary conditions are commonly used, displacement boundary conditions $\vec{u} = \vec{u}_0$, specifying fixed displacement $\vec{u}_0$ along a boundary and traction boundary conditions, $\sigma\vec{n} = \vec{t}_0$, specifying a known traction $\vec{t}_0$ on a boundary surface.

Only two dimensional problems will be considered in this work, using either plane stress or plane strain to reduce the problem to two dimensions. Additional componentwise notations

$$\vec{u} = (u, v) \quad \text{and} \quad \sigma = \begin{bmatrix} \sigma_{xx} & \sigma_{xy} \\ \sigma_{xy} & \sigma_{yy} \end{bmatrix} \tag{11}$$

will be used below for simplicity.

A. Cantilever beam problem

The cantilever beam problem is a standard test case from linear elasticity. An ideal thin beam of length L and height D is bent at one end with force P and kept fixed at the other end. A closed form solution for displacements and stresses under plane stress conditions and a parabolic load on the left side is well known and derived in eg. [17, pp. 284–289]. The beam occupies the region $[0, L]\times[-D/2, D/2]$ and its internal stresses are given as

$$\sigma_{xx} = \frac{Pxy}{I}, \ \sigma_{yy} = 0, \ \sigma_{xy} = \frac{P}{2I}\left(\frac{D^2}{4} - y^2\right), \tag{12}$$

and displacements as

$$\begin{aligned} u &= \frac{Py\left(3D^2(\nu+1) - 4\left(3L^2 + (\nu+2)y^2 - 3x^2\right)\right)}{24EI}, \\ v &= -\frac{P\left(3D^2(\nu+1)(L-x) + 4(L-x)^2(2L+x) + 12\nu x y^2\right)}{24EI}, \end{aligned} \tag{13}$$

where $I = \frac{1}{12}D^3$ is the moment of inertia around the horizontal axis, E is Young's modulus, ν is the Poisson's ratio and P is the total load force.

The problem is solved numerically using RBF-FD and traditional FD methods with traction boundary conditions $\sigma\vec{n} = \vec{t}_0$ given by (12) prescribed on the top, left and bottom boundary, while displacements $\vec{u} = \vec{u}_0$ given by (13) are prescribed on the right boundary. The discretization was regular with equal spacing in both dimensions to enable fair comparison with FD method.

Observed errors of displacements and stresses are measured in relative max-norm

$$e(\vec{u}) = \frac{\max_{x\in X}\{\max|\vec{u}(x) - \hat{\vec{u}}(x)|\}}{\max_{x\in X}\{\max|\vec{u}(x)|\}}, \tag{14}$$

$$e(\sigma) = \frac{\max_{x\in X}\{\max|\sigma(x) - \hat{\sigma}(x)|\}}{\max_{x\in X}\{\max|\sigma(x)|\}}, \tag{15}$$

where $\max|\sigma(x)|$ and $\max|\vec{u}|$ represent the largest element in σ and $\vec{u}$ by absolute value, respectively.

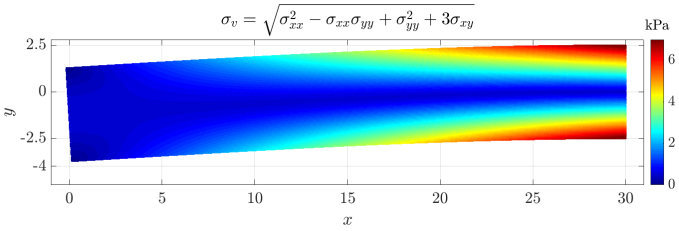

Fig. 2: Von Mises stress σ_v in a deformed cantilever beam. The displacements are magnified by a factor of 10^5 for the sake of visibility.

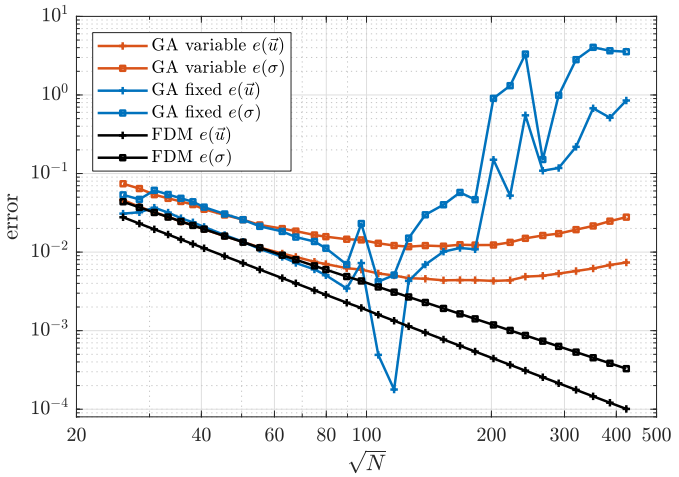

Fig. 3: Errors of RBF-FD and FDM when solving the cantilever beam problem.

The problem was solved with Gaussian RBFs in two different setups. Both setups use Gaussian basis functions with fixed stencil size $n_i = 9$ and one basis function for each stencil node, ie. $m_i = n_i$. First setup uses fixed shape $\varepsilon = 0.01$ and the second uses spatially variable shape $\varepsilon = 0.0025/\delta$, where δ is the distance the closest neighboring node. The most precise numerical solution is shown in Fig. 2 and the errors with respect to the number of nodes is shown in Fig. 3.

The FD method converges regularly with order 2, coinciding with theoretical predictions. The behavior of RBF-FD method also coincides with remarks from section II-C. Using a spatially variable shape parameter ε that is scaled to internodal distance results in a stable method that initially obtains good results, but suffers from stagnation errors later. Using a fixed shape parameter initially produces similar results to the method using variable shape parameter. The errors of both approaches are similar because the shape parameters were chosen in a such a way, that they coincide on initial discretization densities. However, as the node density increases, fixed shape parameter method becomes unstable if naive computation of weights is used, as demonstrated by observed erratic error behavior.

IV. Case arising from fretting fatigue simulations

The fretting fatigue of material is a phenomenon, in which two contact surfaces undergo a small relative oscillatory motion due to cyclic loading. During the simulation of a loading cycle, the stresses in material need to be known, to test for material failure, apply wear damage or initiate crack propagation. One such case, modeling an commonly used experiment in fretting fatigue, is described in [12]. A small thin rectangular specimen of width W, length L and thickness t is stretched in one axis with axial traction σ_{ax} and compressed in another by two oscillating cylindrical pads. The pad's radius of curvature is denoted by R, applied normal force by F and tangential force by Q. The setup is shown in Fig. 4a.

The contact surface is modeled analytically by using an extension of Hertzian contact theory. The theory predicts the contact half-width

$$a = 2\sqrt{\frac{FR}{t\pi E^*}}, \tag{16}$$

where E^* is the combined Young's modulus, given by $\frac{1}{E^*} = \frac{1-\nu_1^2}{E_1} + \frac{1-\nu_2^2}{E_2}$, with E_i and ν_i representing the Young's moduli and Poisson's ratios of the specimen and the pad, respectively. The contact surface is split into stick and slip zones, based on parameters c and e, representing stick zone half-width and eccentricity due to axial loading, respectively, computed as

$$c = a\sqrt{1 - \frac{Q}{\mu f}}, \quad e = \operatorname{sgn}(Q)\frac{a\sigma_{ax}}{4\mu p_0}, \tag{17}$$

where μ is the coefficient of friction and p_0 maximal normal traction, defined below.

Normal traction p is semi-elliptical, defined as

$$p(x) = \begin{cases} p_0\sqrt{1-\frac{x^2}{a^2}}, & |x| \le a \\ 0, & |x| > a \end{cases}, \quad p_0 = \sqrt{\frac{FE^*}{t\pi R}}, \tag{18}$$

and tangential traction $q(x)$ is defined as

$$q(x) = \begin{cases} -\mu p(x) + \frac{\mu p_0 c}{a}\sqrt{1-\frac{(x-e)^2}{c^2}}, & |x-e| < c, \\ -\mu p(x), & c \le |x-e|, |x| \le a, \\ 0, & |x| > a. \end{cases} \tag{19}$$

Some additional inequalities between above quantities must hold in order for p and q to be well defined, all of which are satisfied in our case.

Because of high stresses present, plane strain is used to reduce the problem to two dimensions. Furthermore, symmetry along the horizontal axis is used to halve the problem size. Domain $\Omega = [-L/2, L/2] \times [-W/2, 0]$ therefore has height equal to half the specimen height and is used for numerical simulations in this section. The boundary conditions used are illustrated in Figure 4b. Note that symmetry boundary conditions are used on the bottom boundary.

To ensure comparability with results from [12], matching same parameters values were used. Values of $E_1 = E_2 = 72.1\,\mathrm{GPa}$, $\nu_1 = \nu_2 = 0.33$ were taken for the material parameters, coinciding with aluminum 2420-T3 used in the experiment. Dimensions of the specimen were $L = 40\,\mathrm{mm}$, $W = 10\,\mathrm{mm}$ and $t = 4\,\mathrm{mm}$. The forces in a state of maximal oscillation were $F = 543\,\mathrm{N}$, $Q = 155\,\mathrm{N}$, $\sigma_{ax} = 100\,\mathrm{MPa}$. Two different pad sizes, $R = 10\,\mathrm{mm}$ and $R = 50\,\mathrm{mm}$ were used, and two different coefficients of friction, $\mu = 0.3$ and $\mu = 2$ are chosen for model parameters.

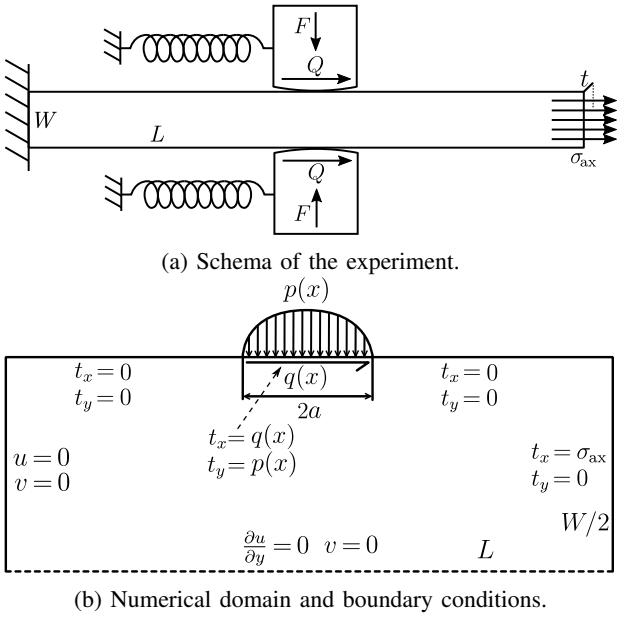

(a) Schema of the experiment.

(b) Numerical domain and boundary conditions.

Fig. 4: Case description. Ratios in drawings are not to scale.

This means that half-contact width a in $R = 10\,\mathrm{mm}$ case equals $0.2067\,\mathrm{mm}$, which is approximately 200 times smaller than domain length L, making it unfeasible to solve without refinement.

The results of the RBF-FD method were compared to a Finite Element Method (FEM) solution, obtained from a commercially available finite element analysis (FEA) software ABAQUS® on four combinations of pad radii and coefficients of frictions specified above. The boundary tractions p and q for all 4 cases are shown in Fig. 5. The cases exhibit different behavior, especially with respect to the coefficient of friction μ, which greatly influences the stick zone size.

The meshes used for FEM solving were refined manually, specifying smaller element size around the contact area with linearly increasing sizes towards the outer edges. A sample mesh is shown in Fig. 6, along with a zommed-in portion, where extensive refinement under contact can be observed. The nodes for RBF-FD discretization were taken from the FEM mesh. The closest 25 nodes were used for stencils and 25 Gaussian basis functions with a varying shape parameter $\varepsilon = 0.0066\delta$ were used for all simulations.

One quantity of interest is the surface stress σ_{xx}, as it has been reported that the peak surface stress is potential point of failure where cracks start to form [12]. The surface stresses for all four cases are shown in Fig. 7. Subsurface von Mises stress for $R = 10\,\mathrm{mm}$ and $\mu = 0.3$ case is shown in Fig. 8.

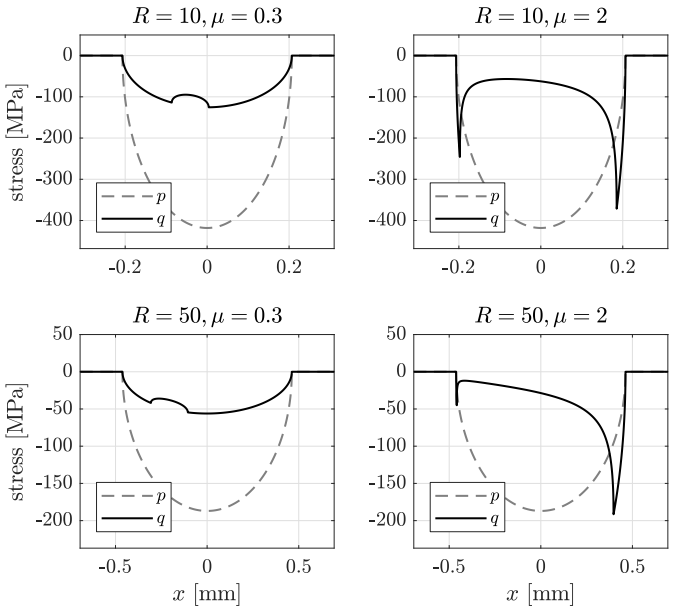

Fig. 5: Tractions p and q on the top boundary for four different cases.

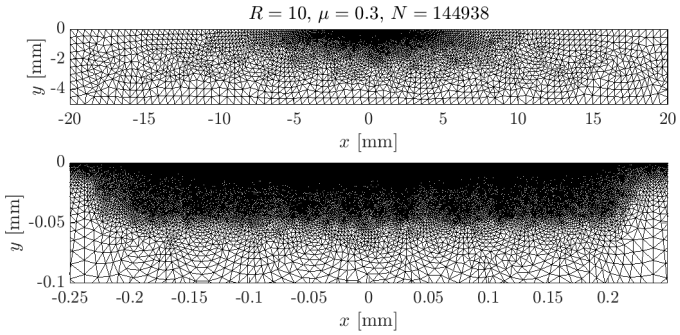

Fig. 6: A sample mesh on $N = 144938$ nodes.

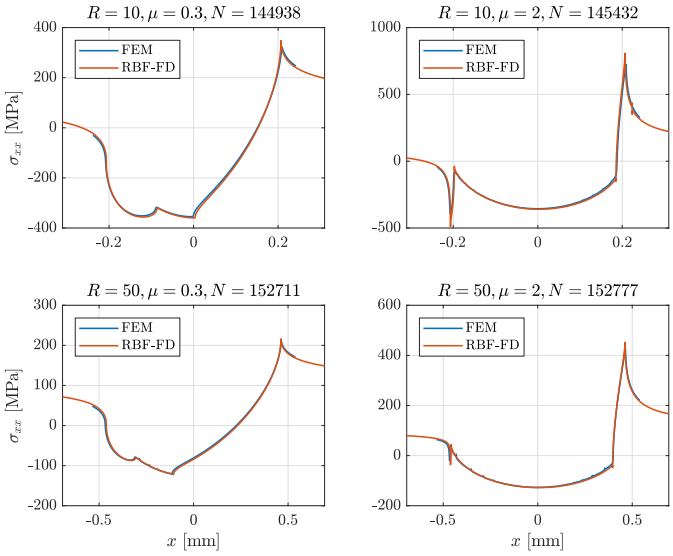

Fig. 7: Surface tractions σ_{xx} computed by FEM and RBF-FD.

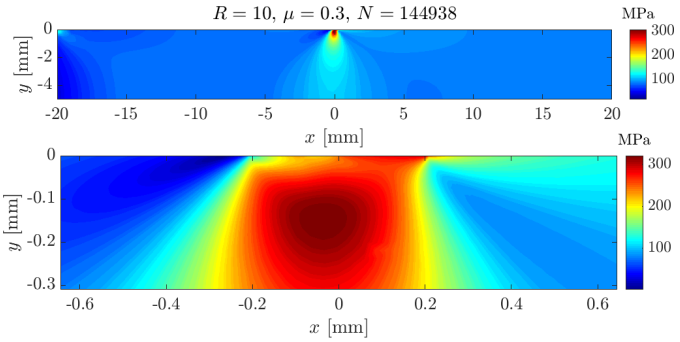

Fig. 8: Subsurface von Mises stress computed by RBF-FD.

V. Conclusion

The paper presents a RBF-FD solution of a linear elastic case arising from fretting fatigue simulations on a refined domain, extending the present use cases of RBF-FD. It is demonstrated that the RBF-FD method gives satisfying results when compared to a commercial FEA software, even when the shape parameter is scaled with internodal distance. Therefore, this stabilization option should be the first to try, as it is the cheapest and easiest, and often results in an adequate numerical solution. Along with ease of implementation, this makes RBF-FD an attractive alternative for solving problems where high variations in node densities are present.

Future work includes extending the method to three-dimensional cases and investigating the benefits of using more stable algorithms for computation of stencil weights.

Acknowledgment

The authors would like to acknowledge the financial support of the Research Foundation Flanders (FWO), The Luxembourg National Research Fund (FNR) and Slovenian Research Agency (ARRS) in the framework of the FWO Lead Agency project: G018916N Multi-analysis of fretting fatigue using physical and virtual experiments and the ARRS research core funding No. P2-0095.

References

[1] R. L. Hardy, "Multiquadric equations of topography and other irregular surfaces," *Journal of geophysical research*, vol. 76, no. 8, pp. 1905–1915, 1971.

[2] C. A. Micchelli, "Interpolation of scattered data: distance matrices and conditionally positive definite functions," in *Approximation theory and spline functions*. Springer, 1984, pp. 143–145.

[3] M. D. Buhmann, *Radial basis functions: theory and implementations*. Cambridge university press, 2003, vol. 12.

[4] E. J. Kansa, "Multiquadrics—A scattered data approximation scheme with applications to computational fluid-dynamics—I surface approximations and partial derivative estimates," *Computers & Mathematics with applications*, vol. 19, no. 8-9, pp. 127–145, 1990.

[5] ——, "Multiquadrics—A scattered data approximation scheme with applications to computational fluid-dynamics—II solutions to parabolic, hyperbolic and elliptic partial differential equations," *Computers & mathematics with applications*, vol. 19, no. 8-9, pp. 147–161, 1990.

[6] C. Franke and R. Schaback, "Solving partial differential equations by collocation using radial basis functions," *Applied Mathematics and Computation*, vol. 93, no. 1, pp. 73–82, 1998.

[7] E. Oñate, F. Perazzo, and J. Miquel, "A finite point method for elasticity problems," *Computers & Structures*, vol. 79, no. 22-25, pp. 2151–2163, 2001.

[8] J. C. Mairhuber, "On Haar's theorem concerning Chebychev approximation problems having unique solutions," *Proceedings of the American Mathematical Society*, vol. 7, no. 4, pp. 609–615, 1956.
[9] P. Curtis, "N-parameter families and best approximation," *Pacific Journal of Mathematics*, vol. 9, no. 4, pp. 1013–1027, 1959.
[10] A. Tolstykh and D. Shirobokov, "On using radial basis functions in a "finite difference mode" with applications to elasticity problems," *Computational Mechanics*, vol. 33, no. 1, pp. 68–79, 2003.
[11] B. Fornberg and N. Flyer, "Solving PDEs with radial basis functions," *Acta Numerica*, vol. 24, p. 215–258, May 2015.
[12] K. Pereira, S. Bordas, S. Tomar, R. Trobec, M. Depolli, G. Kosec, and M. Abdel Wahab, "On the convergence of stresses in fretting fatigue," *Materials*, vol. 9, no. 8, p. 639, 2016.
[13] J. Slak and G. Kosec, "Refined Meshless Local Strong Form solution of Cauchy–Navier equation on an irregular domain," *Engineering Analysis with Boundary Elements*, 2018.
[14] V. Bayona, N. Flyer, B. Fornberg, and G. A. Barnett, "On the role of polynomials in RBF-FD approximations: II. Numerical solution of elliptic PDEs," *Journal of Computational Physics*, vol. 332, pp. 257–273, 2017.
[15] N. Flyer, B. Fornberg, V. Bayona, and G. A. Barnett, "On the role of polynomials in RBF-FD approximations: I. Interpolation and accuracy," *Journal of Computational Physics*, vol. 321, pp. 21–38, 2016.
[16] B. Fornberg, E. Larsson, and N. Flyer, "Stable computations with Gaussian radial basis functions," *SIAM Journal on Scientific Computing*, vol. 33, no. 2, pp. 869–892, 2011.
[17] W. S. Slaughter, *The Linearized Theory of Elasticity*. Birkhäuser Boston, 2002.